# Flow Visualization and Characteristics of a Coaxial Jet with a Tabbed Annular Nozzle*

Takahiro KIWATA**, Takashi ISHII***, Shigeo KIMURA****,
Atsushi OKAJIMA† and Katsuya MIYAZAKI**

Flow visualization and measurements of mean and fluctuating velocities were performed on a coaxial jet with a velocity ratio of 0.6 at a Reynolds number of 3 000 in an open water tank using hot-film anemometry, particle image velocimetry (2D and stereoscopic PIV) and laser-induced fluorescence (LIF). Axisymmetric and streamwise vortical structures were revealed in the near-field of the coaxial jet. The annular nozzle has six vortex generators in order to enhance the streamwise vortices generated in the mixing layer. Furthermore, the annular jet was excited by a shaker in order to enhance the axisymmetric vortices. For the tabbed coaxial jet, jet spreading downstream was greater than for the jet without tabs. The cause of the entrainment increment is the development of axisymmetric and streamwise vortex structures. In the case of excited jets, significant axisymmetric and streamwise vortical structures develop, and the jet width expands from the exit nozzle. Consequently, the flow rate of the excited jet with tabs is larger than that of the unexcited jet without tabs.

***Key Words***: Coaxial Jet, Tabbed Nozzle, Excitation, Mixing Control, Flow Visualization, PIV

## 1. Introduction

The vortical structures in a jet are important for the control of aerodynamic noise and the enhancement or suppression of flow mixing. These three-dimensional structures consist of axisymmetric and streamwise vortices, and interact with each other. As indicated in the investigation of Zaman and Raman[1], both the axisymmetric and streamwise vorticities are of equal importance to the jet mixing process and they are not independent of each other.

There are two techniques to enhance jet mixing: active control and passive control. For active control, an oscillation is usually given to the jet by means of a speaker or a piston. The responses of the coaxial jet upon acoustic excitation were studied by Lepicovsky et al.[2], Tang and Ko[3),(4)] and Wicker and Eaton[5]. Furthermore, the previous work of the authors[6)–(8)] examined the effects of the excitation frequency and the forced excitation of either outer or inner jets on the vortical structure. The exit shape of the jet is altered in order to passively enhance the three-dimensionality of the flow, and thus entrainment and mixing, there have been many efforts devoted to investigating the properties of jets emerging from non-circular nozzles. For example, using a tabbed nozzle generates streamwise vortices in the jet flow, and several studies have reported results for variations in flow field conditions, as well as tab shape, size, number and angle (Ahuja and Brown[9], Bradbury and Khadem[10], Samimy et al.[11], Zaman et al.[1),(12),(13)], Grinsten et al.[14], Toyoda et al.[15]).

In the present work, the interaction between axisymmetric and streamwise vortices in the unexcited and excited coaxial jet was studied experimentally. The annular nozzle has six vortex generators in order to enhance the streamwise vortices generated in the mixing layer. We present results of the flow visualization of the three-dimensional vortical structures and the flow characteristics of the tabbed coaxial jet with a velocity ratio of 0.6 at

* Received 26th February, 2006 (No. 06-4056)
** Graduate School of Natural Science and Technology, Kanazawa University, Kakuma-machi, Kanazawa 920–1192, Japan.
E-mail: kiwata@t.kanazawa-u.ac.jp
*** NACHI-FUJIKOSHI CORP., 1–1–1 Fujikoshi-honmachi, Toyama 930–8511, Japan
**** Institute for Nature and Environmental Technology, Kanazawa University, Kakuma-machi, Kanazawa 920–1192, Japan
† Kanazawa-Gakuin Tanki University, 10 Sue-machi, Kanazawa 920–1392, Japan

a Reynolds number of 3 000.

**Nomenclature**

$a_f$ : amplitude of disturbance velocity
$b_i$ : lip thickness of inner nozzle, i.e., central nozzle
$D_i$ : inner diameter of inner nozzle
$D_o$ : outer diameter of outer nozzle, i.e., annular nozzle
$f$ : vortex frequency
$f_n$ : natural frequency, i.e., the initial vortex frequency of the unexcited jet
$f_e$ : excitation frequency
$Q$ : flow rate
$Re$ : Reynolds number based on $D_o$ and $U_o$
$x$ : axial coordinate
$r$ : radial coordinate
$t$ : time
$\Delta t$ : time interval
$u'$ : axial fluctuating velocity
$v'$ : radia fluctuating velocity
$U_i$ : mean exit bulk velocity of the inner jet
$U_o$ : mean exit bulk velocity of the outer jet
$U_i/U_o$ : velocity ratio
$\delta^*$ : boundary layer displacement thickness

## 2. Apparatus and Experimental Techniques

### 2.1 Experimental setup

As shown in Fig. 1, the experimental setup consists of coaxial axisymmetric water jet discharging into an open tank (435 mm × 435 mm × 100 mm) where the fluid (water) is at rest. Two constant head tanks were used to supply water flow for the outer and the inner nozzle. The flow rate was maintained at a prescribed value by valves and electro-magnetic flowmeters. A schematic diagram of the coaxial nozzle is shown in Fig. 2. The annular and central nozzles are made of acrylic resin. The outer nozzle, i.e., an annular nozzle, has an outer diameter $D_o$ of 40 mm and an inner diameter of 24 mm. In order to enhance the generation of streamwise vortices, six semielliptic tabs (5 mm × 4 mm × 10 mm) were placed at the nozzle exit on the outer side wall of the outer nozzle. These tabs blocked about 9% of the area of the outer nozzle. The inner nozzle has an inner diameter $D_i$ of 16 mm. The pipe is sufficiently long to yield fully developed velocity profiles at the exit plane of the inner jet. The experiments were run with a mean exit bulk velocity $U_o$ of the outer annular jet of about 8 cm/s. The Reynolds number based on the outer diameter, $D_o$, and the mean velocity, $U_o$, of the annular jet was 3 000. The mean velocity ratio was fixed at $U_i/U_o = 0.6$, where $U_i$ is the mean exit bulk velocity of the inner circular jet. The value of boundary layer displacement thickness at the inner side of the outer jet, $\delta^*$ was approximately 1.4 mm.

The sinusoidal motion of the shaker, which consists of a stepping motor and a crank, actuated a piston in a cylinder containing water. A disturbance velocity of amplitude $a_f = 0.1U_o$ was added to the outer jet. The frequency of forced excitation, $f_e$, was $f_n$, where $f_n$ is the initial vortex frequency of the unexcited coaxial jet in the mixing layer, i.e., lip wake vortex frequency[7].

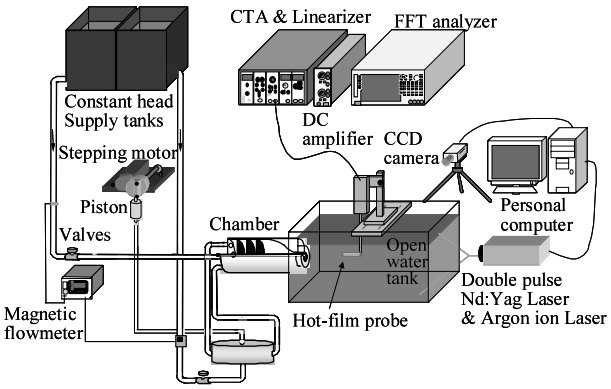


Fig. 1 Schematic sketch of the experiment facility

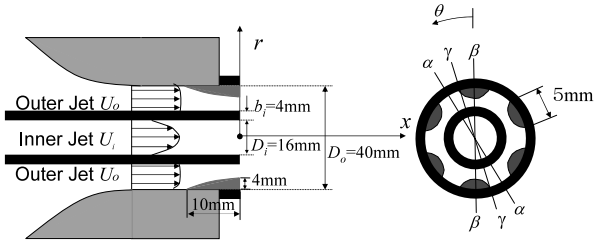


(a) Nozzle (b) Configuration of tabs

Fig. 2 Schematic diagram of the coaxial nozzle

### 2.2 Experimental method

The vortical structure in the near-field was visualized with a two-color planar laser-induced-fluorescence (LIF) technique. A laser sheet was irradiated with a 4 W Argon ion laser (Stabilite2017, Spectra-Physics) to illuminate the near field of the jet. The inner jet and the tank fluids were marked with two different laser-fluorescent dyes, i.e., a fluorescent yellowish-orange dye (aqueous solution of Rhodamine B) and a fluorescent yellowish-green (aqueous solution of disodium fluorescence), respectively. The fluid of the outer jet contained no dye and appears black in the photographs. The photographs were captured from movies recorded via digital video camera (DSR-40, SONY) at a frame rate of 30 Hz for a total time of 20 seconds.

Fluctuating velocities were measured with single-wire probes and hot-film anemometers of constant-temperature type with linearized output. Turbulence quantities and spectrum analyses were done using an FFT analyzer (CF-5210, ONO SOKKI).

For the particle image velocimetry technique (PIV), the fluid was seeded with 20 μm acrylonitrile spherical particles. A light sheet generated with a double-pulse Nd:YAG laser (Big Sky Laser Technologies) illuminated the near field of the jet. The continuous image pairs, up to

200 frames at a framing frequency of 8 Hz, were acquired at 1 599 × 1 185 pixel resolution with a CCD video camera (FlowSense M2 10 bit, Dantec Dynamics). The CCD cameras and double-pulse laser were connected to a computer (CPU: Pentium 4, 3.0 GHz, Memory: 2.0 GB RAM, Hard Disk: 460 GB, DELL), which controlled the timing of the illumination and CCD camera data acquisition; velocimetry was calculated with those images. Figure 3 shows the schematic setup of the stereoscopic PIV system used in the present study. Two prisms were used to keep out refraction. The two CCD cameras were arranged in an angular displacement configuration in order to obtain the three velocity components in the illuminating laser sheet plane. The lenses and camera bodies were adjusted to satisfy Scheimpflug condition to obtain focused particle images everywhere in the image recording planes, and the angle between the viewing axes of the cameras is about 90 degrees. The time interval between the two pulsed illuminations, $\Delta t$, was set at 3.5 ms. The spatial resolution was approximately 0.087 mm/pixel.

## 3. Results and Discussion

### 3.1 Unexcited jet

Figure 4 shows flow patterns in $x$-$r$ cross-sections. For the tabbed coaxial jet, two flow patterns were taken at $\alpha$ and $\beta$ cross-sections, as shown in Fig. 2 (b). The vortices in the inner and outer shear layers of the coaxial jet without tabs (Fig. 4 (a)) form an alternating array; with each of the vortices being convected downstream without vortex pairing. Because the vortices in the outer shear layer roll up, the vortices in the inner shear layers are no longer identifiable as separate entities beyond $x/D_o = 2.0$. For the coaxial jet with tabs, the vortices in the outer shear layer at an $\alpha$ cross-section (Fig. 4 (b)) are observed in the downstream after $x/D_o = 1.5$. Although the jet width at a $\beta$ cross-section shrinks due to the tabs (Fig. 4 (c)), the location of vortex formation at a $\beta$ cross-section is closer to the nozzle exit than that at $\alpha$ cross-section. It seems that the two fluid streams of the outer and inner jets do not mix well for the unexcited coaxial jet with tabs.

Figure 5 shows cross-sections of the coaxial jet, cut into round slices by the laser sheet at distances $x/D_o = 0.5$, 1.5 and 2.5 from the nozzle exit. These figures show the jet with and without tabs, respectively. The cross-sectional flow pattern of the jet without tabs at $x/D_o = 0.5$ shows approximate circles that are concentric with the coaxial rings of the outer jet (black portion in Fig. 5 (a)) and the inner jet. At $x/D_o = 1.5$, the yellowish-orange inner jet spreads to the ambient fluid; it turns out that the outer jet rolls up the inner jet, as shown in Fig. 4 (a). At $x/D_o = 2.5$, the jet boundary was no longer circular, and the streamwise vorticity was well developed. For the coaxial jet with tabs (Fig. 5 (b)), it can be seen that the configuration of the tabbed jet at $x/D_o = 0.5$ has the same shape as the tabbed nozzle geometry. The shape of the vortical structure in the outer jet at $x/D_o = 1.5$ becomes distorted like a flower, and the evolution of streamwise vortices is revealed. At $x/D_o = 2.5$, the many small streamwise vortices evolved further, due to flow instability. However, it seems that the inner jet is surrounded by the outer jet without mixing. Therefore, both streamwise and axisymmetric vorticities are connected to each other, indicating that three-dimensional effects are of prime importance for the vertical structure. It is evident that streamwise vortices prevent the evolution of axisymmetric vortices.

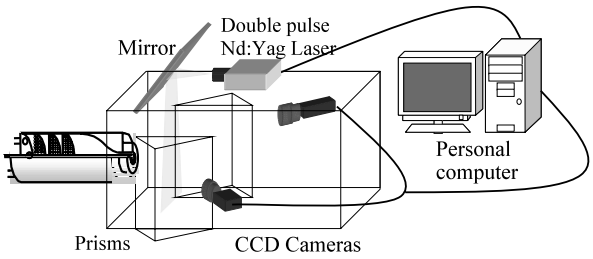


Fig. 3 Schematic diagram of the stereoscopic PIV facility

Continuous color contours of the streamwise mean velocity measured by PIV are shown in Fig. 6. For the coaxial jet without tabs (Fig. 6 (a)), the annular jet flows inward towards the jet axis and merges near $x/D_o = 1.75$. On the other hand, the high mean velocity of the tabbed coaxial jet at an $\alpha$ cross-section is distributed parallel to the jet axis (Fig. 6 (b)). As shown in Fig. 6 (c) for a $\beta$ cross-section, the flow from the annular nozzle is contracted due to the height of the tabs. The mean axial velocity distribution along the centerline is also presented in Fig. 7. The centerline velocity of the jet with tabs was not attenuated, as compared to the jet without tabs. It seems that the two fluid streams of the outer and inner jets do not mix well. Note that the spread of the velocity of the jet with tabs downstream is greater than that of the jet without tabs.

The contours for r.m.s. values of the streamwise velocity fluctuations are depicted in Fig. 8. For the tabbed jet at an $\alpha$ cross-section, high velocity fluctuations are distributed in the outer mixing region. The velocity fluctuation near the centerline is smaller than that of the jet without tabs. The decrease in velocity fluctuation is due to the absence of roll-up vortices in the inner shear layer.

Figure 9 shows instantaneous vorticity contours. For the jet without tabs, the vortical structures in the outer and inner shear layers were symmetric about the centerline of the jet. For the tabbed jet at an $\alpha$ cross-section, the vorticity in the inner shear layer was weak as compared to the jet without tabs. Similarly, the velocity fluctuation was small near the centerline, as shown in Fig. 8 (b). The shedding vortex in the outer shear layer spreads from $x/D_o = 1.5$. Furthermore, for the tabbed jet at a $\beta$ cross-section, the vorticity in the outer shear layer is also weak.

The velocity fluctuations in the near field of the coax-

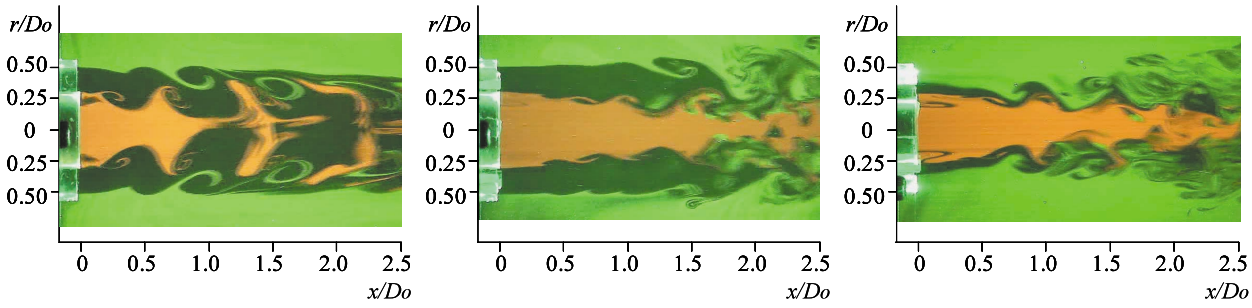


(a) Without tabs (b) With tabs ($\alpha$ cross-section) (c) With tabs ($\beta$ cross-section)

Fig. 4 Visualized flow patterns in $x$-$r$ cross-sections for the unexcited jet

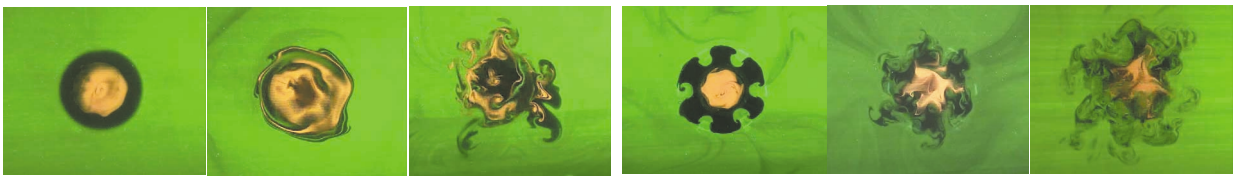


(a) Without tabs (b) With tabs

Fig. 5 Visualized flow patterns at $r$-$\theta$ cross sections for the unexcited jet

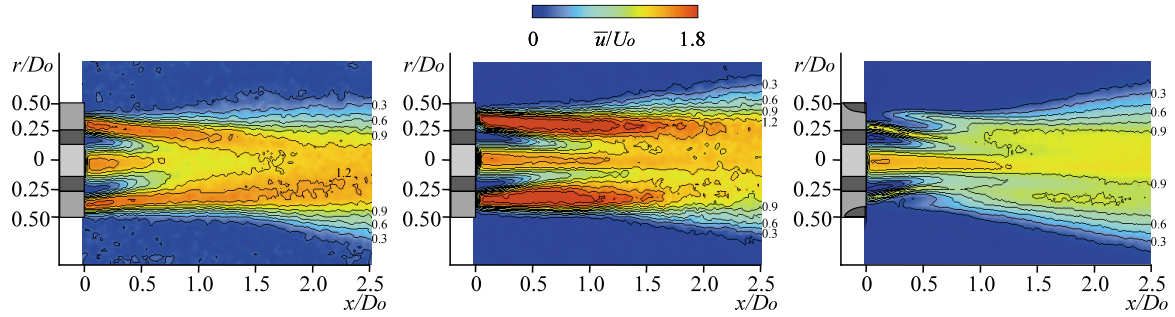


(a) Without tabs (b) With tabs ($\alpha$ cross-section) (c) With tabs ($\beta$ cross-section)

Fig. 6 Mean axial velocity contours for the unexcited jet

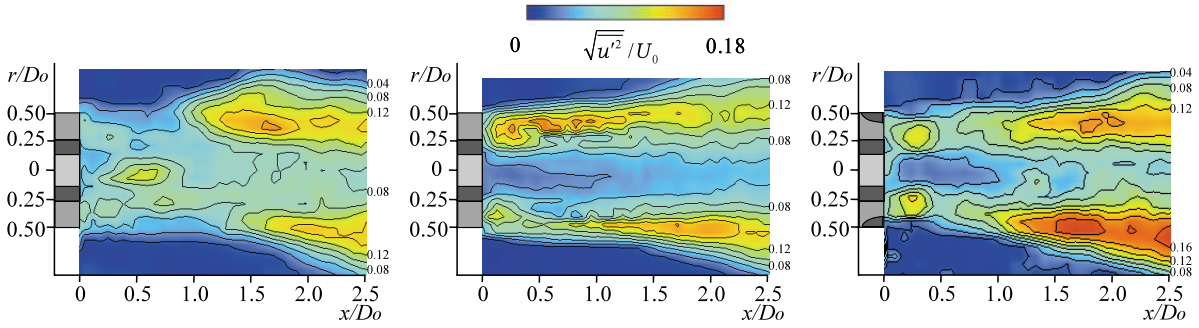


(a) Without tabs (b) With tabs ($\alpha$ cross-section) (c) With tabs ($\beta$ cross-section)

Fig. 8 Contours of streamwise velocity fluctuation RMS values for the unexcited jet

ial jet were spectrally analyzed. Figure 10 shows the streamwise variations in spectra of $u'$ signal in the inner mixing region at $r/D_o = 0.25$. For the jet without tabs (Fig. 10 (a)), a peak of the fundamental component $f_n \approx 3.0$ Hz remains until $x/D_o = 2.0$. Its component is the lip wake vortex frequency[7]. The subharmonic component $f_n/2$ is observed at $r/D_o \geq 1.5$, but these spectra exhibit a broad peak around $f \approx 1.5$ Hz. On the other hand, a predominant spectrum peak for the jet with tabs is not observed after the nozzle exit. It is inferred from the flow patterns in Fig. 4 (b) and (c).

### 3.2 Excited jet

Figure 11 shows the flow patterns in different $x$-$r$ cross-sections for the excited jet. These figures compare the excited jet with and without tabs. The large growth of vortices in the outer shear layer of the excited jet is observed from the near field of the nozzle as compared with the unexcited jet shown in Fig. 4. For the excited case with tabs, a small vortical structure is seen in the mixing regions, and their vortices in the outer shear layer are convected outward towards the jet axis. Excited coaxial jet cross-section flow patterns, cut into round slices by the laser sheet at distances $x/D_o = 0.5$ and 1.5, are also shown in Fig. 12. For the excited jet without tabs at $x/D_o = 0.5$, a weak streamwise vortical structure (yellowish-orange) is formed in the inner shear layer. Downstream at $x/D_o = 1.5$, a streamwise vortical structure develops, unlike the case of the excited jet without tabs shown in Fig. 12 (b). For the excited jet with tabs, the streamwise vortical structure is formed rapidly. For the excited jet with tabs at $x/D_o = 1.5$, it seems that the inner jet (yellowish-orange) does not spread fully until reaching the ambient fluid (yellowish-green) in the same manner as the unexcited jet with tabs, while the jet width of the excited jet was larger than that of the unexcited jet downstream (not shown here).

The streamwise mean velocity and radial velocity fluctuation contours are shown in Figs. 13 and 14, respectively. For the excited jet with tabs, jet spreading increases as compared to the unexcited jet with tabs (Fig. 6 (b) and (c)). It seems that the turbulent intensity mainly increases from the nozzle exit in the outer mixing region due to the streamwise vortical structure generated by the forced excitation. But the turbulent intensity in the inner mixing

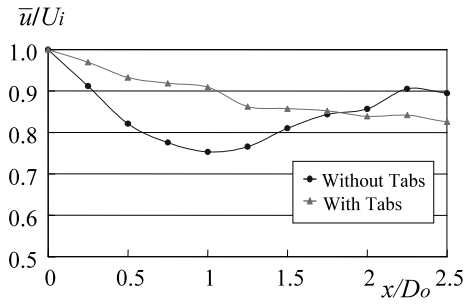


Fig. 7 Variation in axial velocity along centerline for the unexcited jet

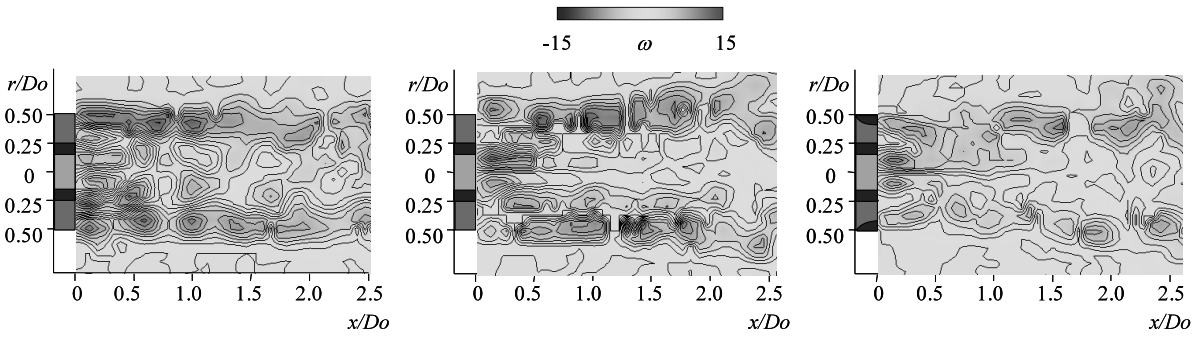


(a) Without tabs (b) With tabs ($\alpha$ cross-section) (c) With tabs ($\beta$ cross-section)

Fig. 9 Instantaneous vorticity contours for the unexcited jet

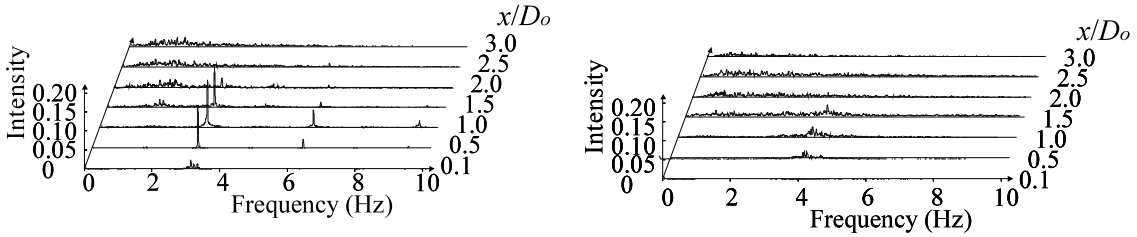


(a) Without tabs (b) With tabs ($\alpha$ cross-section)

Fig. 10 Streamwise variation in velocity fluctuation signal spectra for the unexcited jet ($r/D_o = 0.25$)

region near the jet axis does not increase. Figure 15 shows instantaneous vorticity contours for the excited jet with tabs at a cross-section. The vorticity in the inner shear-layer was weak as compared to the unexcited jet without tabs (Fig. 9 (a)). The vortex array is mainly formed in the outer shear-layer, their vortices being convected outward toward the jet axis. Thus, the data for the excited jet case with tabs has trends similar to the data for the unexcited

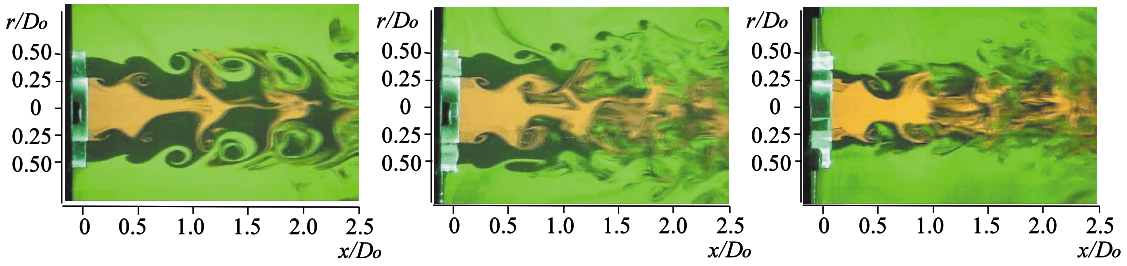


(a) Without tabs (b) With tabs ($\alpha$ cross-section) (c) With tabs ($\beta$ cross-section)

Fig. 11 Visualized flow patterns at $x$-$r$ cross-sections for the excited jet

Without tabs With tabs Without tabs With tabs

(a) $x/D_o = 0.5$ (b) $x/D_o = 1.5$

Fig. 12 Visualized flow patterns at $r$-$\theta$ cross-sections at $x/D_o = 0.5$ and 1.5 for the excited jet

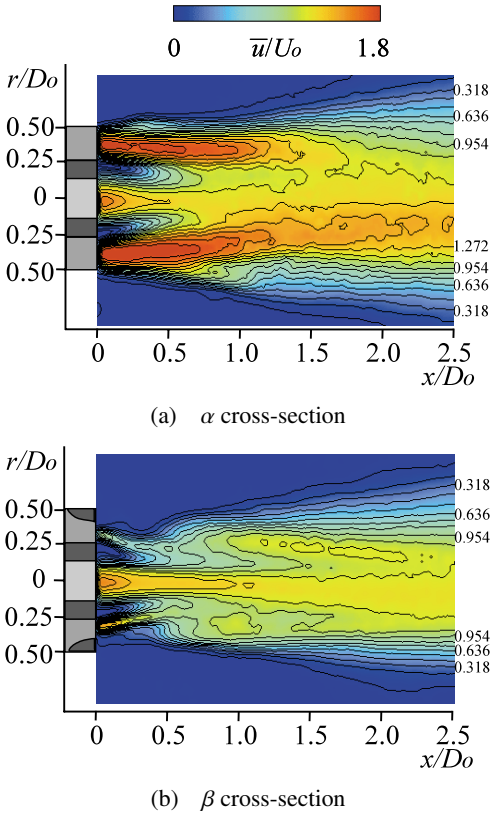


(a) $\alpha$ cross-section

(b) $\beta$ cross-section

Fig. 13 Mean axial velocity contours for the excited jet with tabs

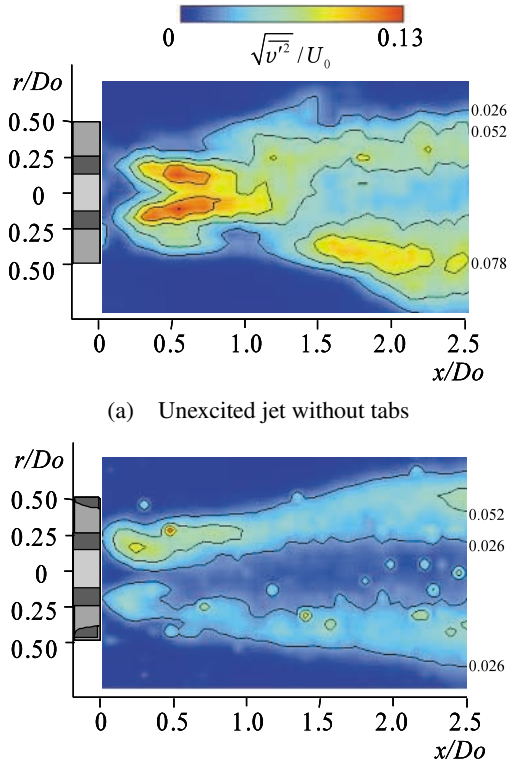


(a) Unexcited jet without tabs

(b) Excited jet with tabs ($\beta$ cross-section)

Fig. 14 R.M.S. values of radial velocity fluctuations contours

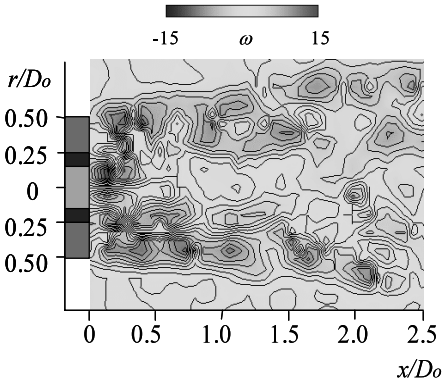


Fig. 15 Instantaneous vorticity contours for the excited jet with tabs at an $\alpha$ cross-section

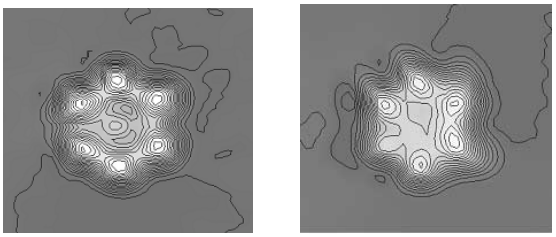

$x/D_o$=0.5 $x/D_o$=1.5

(a) Unexcited jet with tabs

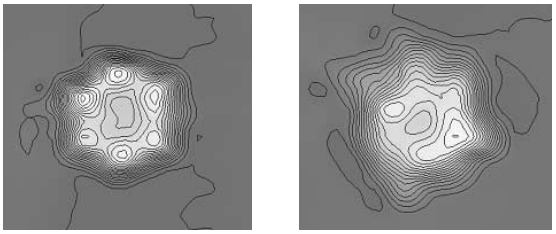

$x/D_o$=0.5 $x/D_o$=1.5

(b) Excited jet with tabs

Fig. 16 Mean axial velocity contours at $r$-$\theta$ cross sections

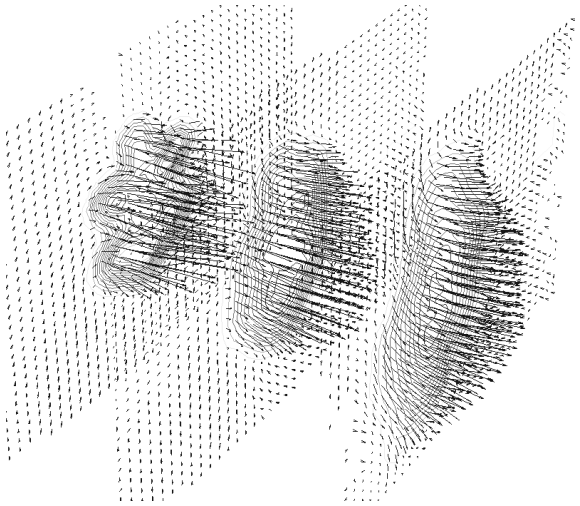

(a) Unexcited jet with tabs

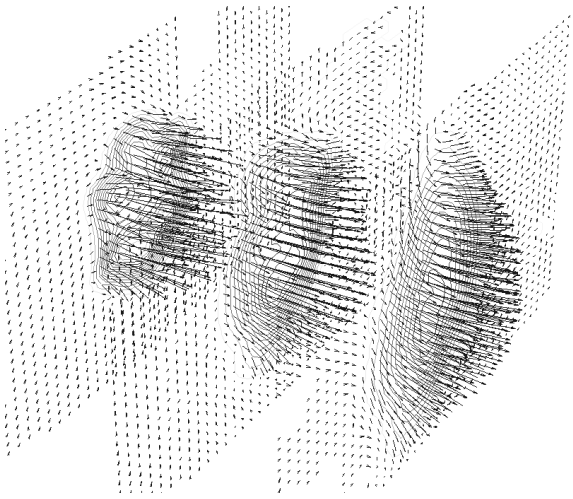

(b) Excited jet with tabs

Fig. 17 Three-dimensional velocity vectors at $x/D_o = 0.5$, 1.5 and 2.5 cross-sections for the tabbed coaxial jet

jet with tabs.

### 3.3 Streamwise variation of three-dimensional velocity distributions and flow rate

Mean axial velocity contours and the three-dimensional velocity vectors at different $r$-$\theta$ cross-sections measured by the stereoscopic PIV system are shown in Figs. 16 and 17, respectively. A three-dimensional visual impression of the jet spreading for each case can be obtained from Fig. 17. For the coaxial jet with tabs, there are six local velocity maxima in the $r$-$\theta$ cross-section at $x/D_o = 0.5$. The signature of the tabbed nozzle in a form of six-tabbed structure can still be identified downstream at $x/D_o = 1.5$ for the unexcited jet. However, for the excited jet with tabs, a developed velocity profile can be seen in Fig. 17 (b) over $x/D_o = 1.5$. The increase in jet spreading is thought to be a result of the mixing between the excited outer jet with tabbed nozzle and the ambient fluid.

The axial distributions of jet flow rate are plotted in

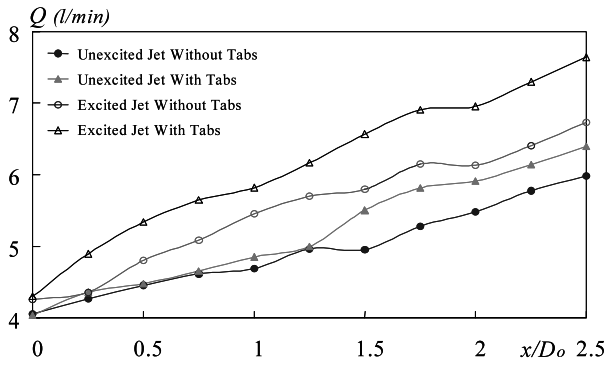


Fig. 18 Streamwise variation in flow rate

Fig. 18. The flow rate $Q$ is defined as the integrated value of the velocity profile to the radial location of $0.1U_{\max}$, where $U_{\max}$ is the maximum velocity in each axial plane. The tabbed jet flow rate takes an average flow rate using velocity profiles at $\alpha$, $\beta$ and $\gamma$ cross-sections, as shown in

Fig. 2 (b). For the unexcited jet, the flow rates with and without tabs are approximately equal until $x/D_o = 1.25$. For $x/D_o \geq 1.25$, the tabbed jet flow rate increases more than that of the jet without tabs. The cause of the entrainment increment is the development of streamwise vortices; the jet width expands from $x/D_o = 1.5$ as shown in Fig. 6 (b) and (c). In the case of excited jets, significant axisymmetric and streamwise vortical structures develop, and the jet width expands from the exit nozzle. Consequently, the flow rate of the excited jet with tabs is larger than that of the unexcited jet without tabs. Downstream for $x/D_o > 1.5$, the entrainment rate of $dQ/dx$ is almost the same in each case.

## 4. Conclusions

The effect of tabs on the flow structure of coaxial jets was studied. The following conclusions can be drawn:

( 1 ) In the case of an unexcited jet with tabs, streamwise vortices evolve from near the jet exit. But the two fluid streams of the outer and inner jets do not mix well, and the turbulent intensity in the inner mixing region is no higher than that of the coaxial jet without tabs. This phenomenon is related to large-scale structures in the mixing region. Axisymmetric vortices in inner shear layer do not form clearly because streamwise vortices caused by the tabs prevent the evolution of axisymmetric vortices.

( 2 ) Streamwise variations in the flow rates of unexcited jets with and without tabs were approximately equal until $x/D_o = 1.25$. For $x/D_o > 1.25$, the flow rate for the tabbed jet increases more than that for the jet without tabs. Downstream, the entrainment rate of $dQ/dx$ is almost the same in each case.

( 3 ) In the case of the excited jet with tabs, the jet is wider than the excited jet without tabs, because streamwise vortices significantly develop from the nozzle exit. It was found that enhanced axisymmetric and streamwise vortex structures increase jet spreading.

## Acknowledgment

The authors are thankful to Dr. Michael Vynnycky, Associate Professor at the Royal Institute of Technology in Stockholm, Sweden, for providing useful comment and discussion, and also acknowledge Mr. Tomohiro Kuratani, Technician at Kanazawa University, for his help with the experiment.

## References

( 1 ) Zaman, K.B.M.Q. and Raman, G., Reversal in Spreading of a Tabbed Circular Jet under Controlled Excitation, Phys. Fluids, Vol.9, No.12 (1997), pp.3733–3740.

( 2 ) Lepicovsky, J., Ahuja, K.K. and Burrin, R.H., Tone Excited Jets, Part III: Flow Measurements, J. Sound Vib., Vol.102 (1985), pp.71–91.

( 3 ) Tang, S.K. and Ko, N.W.M., Coherent Structure Interactions in Excited Coaxial Jet of Mean Velocity Ratio of 0.3, AIAA J., Vol.31, No.8 (1993), pp.1521–1524.

( 4 ) Tang, S.K. and Ko, N.W.M., Experimental Investigation of the Structure Interaction in an Excited Coaxial Jet, Exp. Thermal and Fluid Sci., Vol.8, No.3 (1994), pp.214–229.

( 5 ) Wicker, R.B. and Eaton, J.K., Near Field of a Coaxial Jet with and without Axial Excitation, AIAA J., Vol.32, No.3 (1994), pp.542–546.

( 6 ) Kiwata, T., Okajima, A., Ueno, H. and Kimura, S., Effects of Excitation on Plane and Coaxial Jets, Proc. of 3rd Joint ASME/JSME Fluids Eng. Conf., San Francisco, U.S.A., FEDSM99-6953, (1999), pp.1–8.

( 7 ) Kiwata, T., Okajima, A., Kimura, S. and Ando, K., Flow Visualization of Vortex Structure of an Excited Coaxial Jet, J. Visualization, Vol.4, No.1 (2001), pp.99–107.

( 8 ) Kiwata, T., Okajima, A., Kimura, S. and Ishii, K., Flow Visualization of Excited Coaxial Water Jet with Phase Difference, Proc. 4th ASME-JSME Fluids Eng. Conf., Honolulu, Hawaii, USA, FEDSM03–45230, (2003), pp.1–8.

( 9 ) Ahuja, K.K. and Brown, W.H., Shear Flow Control by Mechanical Tabs, AIAA 2nd Shear Flow Conference, Paper No.89-0994, (1989).

(10) Bradbury, L.J.S. and Khadem, A., The Distortion of a Jet by Tabs, J. Fluid Mech., Vol.70 (Part4) (1975), pp.801–813.

(11) Samimy, M., Reeder, M. and Zaman, K., Supersonic Jet Mixing Enhancement by Vortex Generators, AIAA/SAE/ASME/ASEE 27th Joint Propulsion Conference, Paper No.91-2263, (1991).

(12) Zaman, K.B.M.Q., Streamwise Vorticity Generation and Mixing Enhancement in Free Jets by Delata-Tabs, AIAA Shear Flow Conference, Paper No.93-3253, (1993).

(13) Zaman, K.B.M.Q., Samimy, M. and Reeder, M.F., Control of an Axisymmetric Jet Using Vortex Generators, Phys. Fluids, Vol.6, No.2 (1994), pp.778–793.

(14) Grinstein, F.F., Gutmark, E.J., Parr, T.P., Hanson-Parr, D.H. and Obeysekare, U., Streamwise and Spanwise Vortex Interaction in an Axisymmetric Jet. A Computational and Experimental Study, Phys. Fluid, Vol.8, No.6 (1996), pp.1515–1524.

(15) Toyoda, K., Mori, H. and Hiramoto, R., Dynamics of the Streamwise Vortices in an Axisymmetric Mixing Layer, Proc. 4th ASME-JSME Fluids Eng. Conf. Honolulu, Hawaii, USA, FEDSM2003-45229, (2003), pp.1–8.